Applied Surface Science 311 (2014) 729–733

Contents lists available at ScienceDirect

Applied Surface Science

journal homepage: www.elsevier.com/locate/apsusc

Physical properties of chemically deposited Bi_2S_3 thin films using two post-deposition treatments

H. Moreno-García [a,*], S. Messina [b], M. Calixto-Rodriguez [c], H. Martínez [a]

[a] Instituto de Ciencias Físicas, Laboratorio de espectroscopia, Universidad Nacional Autónoma de México, Apartado Postal 48-3, C.P. 62210 Cuernavaca, Morelos, Mexico
[b] Universidad Autónoma de Nayarit, Ciudad de la Cultura "Amado Nervo" S/N, C.P. 63155 Tepic, Nayarit, Mexico
[c] Universidad Tecnológica Emiliano Zapata del Estado de Morelos, Av. Universidad Tecnológica No. 1, C.P. 62760 Emiliano Zapata, Morelos, Mexico

ARTICLE INFO

Article history:
Received 18 March 2014
Received in revised form 5 May 2014
Accepted 22 May 2014
Available online 2 June 2014

Keywords:
Bismuth sulfide
Thin films
Chemical deposition
Plasma treatment

ABSTRACT

As-deposited bismuth sulfide (Bi_2S_3) thin films prepared by chemical bath deposition technique were treated with thermal annealed in air atmosphere and argon AC plasma. The as-deposited, thermally annealing and plasma treatment Bi_2S_3 thin films have been characterized by X-ray diffraction (XRD) analysis, atomic force microscopy analysis (AFM), transmission, specular reflectance and electrical measurements. The structural, morphological, optical and electrical properties of the films are compared. The XRD analysis showed that both post-deposition treatments, transform the thin films from amorphous to a crystalline phase. The atomic force microscopy (AFM) measurement showed a reduction of roughness for the films treated in plasma. The energy band gap value of the as-prepared film was $E_g = 1.61$ eV, while for the film thermally annealed was $E_g = 1.60$ eV and $E_g = 1.56$ eV for film treated with Plasma. The electrical conductivity under illumination of the as-prepared films was $3.6 \times 10^{-5}\,(\Omega\,\mathrm{cm})^{-1}$, whereas the conductivity value for the thermally annealed films was $2.0 \times 10^{-3}\,(\Omega\,\mathrm{cm})^{-1}$ and for the plasma treated films the electrical conductivity increases up to $7.7 \times 10^{-2}\,(\Omega\,\mathrm{cm})^{-1}$.

1. Introduction

Research in semiconductor thin film materials for application in solar cells have increased in recent decades due to the need to find new abundant and low-toxicity materials, in order to complement current thin film solar cells technologies [1].

One of the features that make a semiconductor material suitable for solar cells applications is its value of the energy band gap (E_g), which must be in the range of 1.1–1.6 eV, as suggested by some theoretical studies about the conversion efficiency for ideal solar cells [2].

Bismuth sulfide (Bi_2S_3) is a semiconductor material with an energy band gap value reported of 1.3 eV (bulk), this feature makes it a good candidate to be used as an absorber material in thin film solar cells [3]. The synthesis of Bi_2S_3 thin films has been reported by many authors, such as: spray pyrolysis [4], electrodeposition [5], vacuum thermal evaporation and chemical bath deposition [6,7], ionic layer adsorption and reaction (SILAR) [8]. Bismuth sulfide thin films obtained by the above mentioned techniques have reported E_g values between 1.9 and 1.52 eV, depending on the deposition method. The electrical conductivity values for Bi_2S_3 thin films are in the range of $8.5 \times 10^{-5}\,(\Omega\,\mathrm{cm})^{-1}$ to $0.2\,(\Omega\,\mathrm{cm})^{-1}$. Furthermore, Bi_2S_3 is used for the development of the ternary compound Cu_3BiS_3 which offers excellent properties as a potential photovoltaic absorber material with high optical efficiency [9]. There are several reports about the application of Bi_2S_3 thin films in photovoltaic devices [10–13]. One of the most prominent photovoltaic devices is composed by Bi_2S_3 nanocrystals and p-type PbS quantum dots with a conversion efficiency of 5.0% [13]. It demonstrates the feasibility of using this material in solar cells application.

The chemical deposition technique is widely known for being a simple and low cost method to obtain uniform thin films, with the advantage of easy scale-up. However, the films produced by this method have very poor crystallinity; so that, post-deposition heat treatments are required in order to improve their structural characteristics. Nair et al. reported that the chemically deposited Bi_2S_3 thin films with a heat treatment in air at 250 °C produces a change of the Bi_2S_3 thin films from amorphous phase to crystalline phase. However, that process yields a significant loss of thickness (about 40%) [10].

It has been reported for some materials, such as: CuS, SnS and Sb_2S_3, that a post-deposition treatment with plasma produces a

* Corresponding author. Tel.: +52 55 5622 7759; fax: +52 55 56 227775.
E-mail addresses: hamog@ier.unam.mx, psishes@gmail.com (H. Moreno-García).

http://dx.doi.org/10.1016/j.apsusc.2014.05.147
0169-4332/

significant enhancement in their optical, electrical and structural properties [14–16]. The plasma treatment represents an alternative post-deposition process in order to modify the physical properties of the films, which could result in photovoltaic devices with better conversion efficiencies.

For this work, we have used chemical bath deposition technique to obtain thin films of Bi_2S_3 [17]. The modification on physical properties of the films, caused by the effect of post-deposition treatments (air annealing at 250 °C for 30 min and Ar plasma) are compared and discussed.

2. Experimental details

2.1. Bi_2S_3 thin films

The reaction solution as well as the deposition conditions were done following the method reported by Nair et al. in Ref. [17], and it is cited below.

For the deposition of the Bi_2S_3 films a reaction solution containing 10 ml of 0.5 M bismuth nitrate dissolved in TEA; 8 ml 1 M thioacetamide and de-ionized water to complete 100 ml volume was prepared [6]. After 105 min of deposition a thin film of Bi_2S_3 about 145 nm in thickness was obtained.

2.2. Air annealing

The as-prepared samples were placed in a Petri dish sealed with teflon tape, in order to prevent the loss of sulfur during the thermal treatment. Subsequently, the films were annealed in air at 250 °C for 30 min.

2.3. Plasma treatment

The system consisted of two circular copper electrodes with 80 mm in diameter and a gap spacing of 3 mm. Electrodes were placed horizontally at the center of the reaction chamber. The samples were placed on bottom electrode. To generate the plasma, argon gas was injected into the chamber. The AC discharge power supply was maintained at 290 V and a current of 64 mA. The samples were treated with the Ar plasma at a pressure of 3 Torr, for 75 min.

3. Characterization

The X-ray diffraction (XRD) patterns of the thin films were measured using a JASCO-670 diffractometer in grazing incident mode ($\Omega = 1°$). The crystal size (D) was calculated by using the computer software of the equipment. The film thickness (d) was recorded using an Ambios Technology measured on an XP-200 thickness measurement unit. For morphology analysis an atomic force microscopy (AFM) Dimension Icon DS100 was used. The NanoScope Analysis software version 1.4 for calculating the root mean square (RMS) roughness was used. The optical transmission measurements are used to determine optical absorption coefficients. Transmission (T) and specular reflectance (R) spectra of the films were measured in the UV–vis–NIR region (200–1100 nm wavelength range), using a spectrophotometer Shimadzu UV1800. The optical absorption coefficient (α) was estimated from the T and R spectra and film thickness (d). The semiconductor energy band gap was determined by measuring the absorption coefficient as a function of the photon energy [20]. For electrical characterization of the samples, two silver paint electrodes were painted on the films surfaces (5 mm long and 5 mm separation). The photoresponse measurements were carried out by maintaining the films on dark, in order to stabilize them in darkness, once, the current was measured in the dark for 30 s with a bias voltage of 5 V, then 30 s under illumination conditions with an intensity of 850 W/m^2 (tungsten – halogen radiation, temperature 3300 K), finally 30 s in the dark. Current data were acquired every second using a measurement system constituted by a programmable voltage source Kiethley 230 and a digital multimeter Keithley 619, linked to a computer. The electrical conductivity in the dark and under illumination, and the conductivity type were determined using the photo-response data of each film [17].

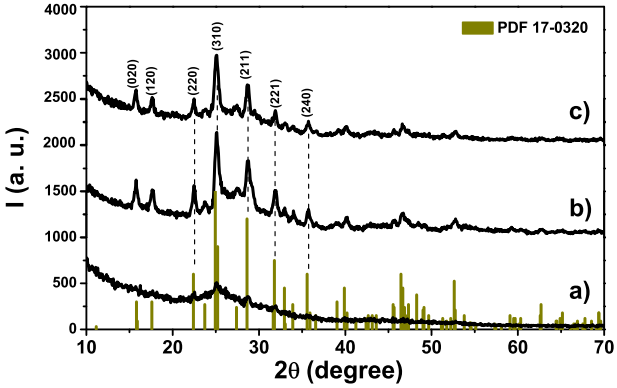

Fig. 1. X-ray diffraction patterns of Bi_2S_3 thin films: (a) as-deposited, (b) annealed in air and (c) treated by Ar plasma.

4. Results and discussion

The thickness (d) measurements of Bi_2S_3 samples were: 145 nm for the as-prepared films; 94 nm for films annealed in air at 250 °C for 30 min and 140 nm for films treated in argon plasma. The annealed in air process produced a loss in thickness of 35% while the film treated in Ar plasma has a loss in thickness of 3%.

4.1. Structural and morphological characterization

The XRD measurements of the Bi_2S_3 thin films as-prepared, annealed in air and treated in Ar plasma are shown in Fig. 1. The XRD patterns of samples subjected to post-deposition treatments were compared with the standard pattern of the orthorhombic crystalline phase for the mineral bismuthinite, PDF # 17-0320. In both cases (annealed in air and treated in plasma), it was observed that the main peak of the XRD spectra corresponds to (3 1 0) diffraction plane, another XRD peaks of both samples match well with those for the crystalline planes (2 0 0), (2 2 0), (2 1 1), (2 2 1) and (2 4 0). Also, the peaks of the sample annealed in air have more intensity than the sample treated in plasma. Furthermore, it can be observed in both cases a better definition of the XRD peaks in the 2θ region of 40–52°. The as-prepared films give an amorphous phase, but their XRD patterns is displayed in Fig. 1 for comparison. The calculated crystal size value (D) for the sample annealed in air is 15.6 nm and 16.5 nm for the sample treated in plasma.

The AFM analysis of the morphology and 3D surface of the Bi_2S_3 as-prepared thin films, thermally annealed in air and treated by Ar plasma are shown in Fig. 2. Through AFM analysis the roughness values were estimated. The as-prepared film has a roughness of 15.6 nm, the film of Bi_2S_3 annealed in air of 24.9 nm and the film treated in plasma of 42.0 nm. A higher impact on the surface is observed for the sample treated by Ar (Fig. 2(e) and (f)) compared with the as-prepared film (Fig. 2(a) and (b)) and annealed in air (Fig. 2(c) and (d)). From literature is known that the application of thin films of Bi_2S_3 with smoother surface morphology improves the device performance in optoelectronic devices like photodiodes [18]. Hence, as the film surface obtained after plasma

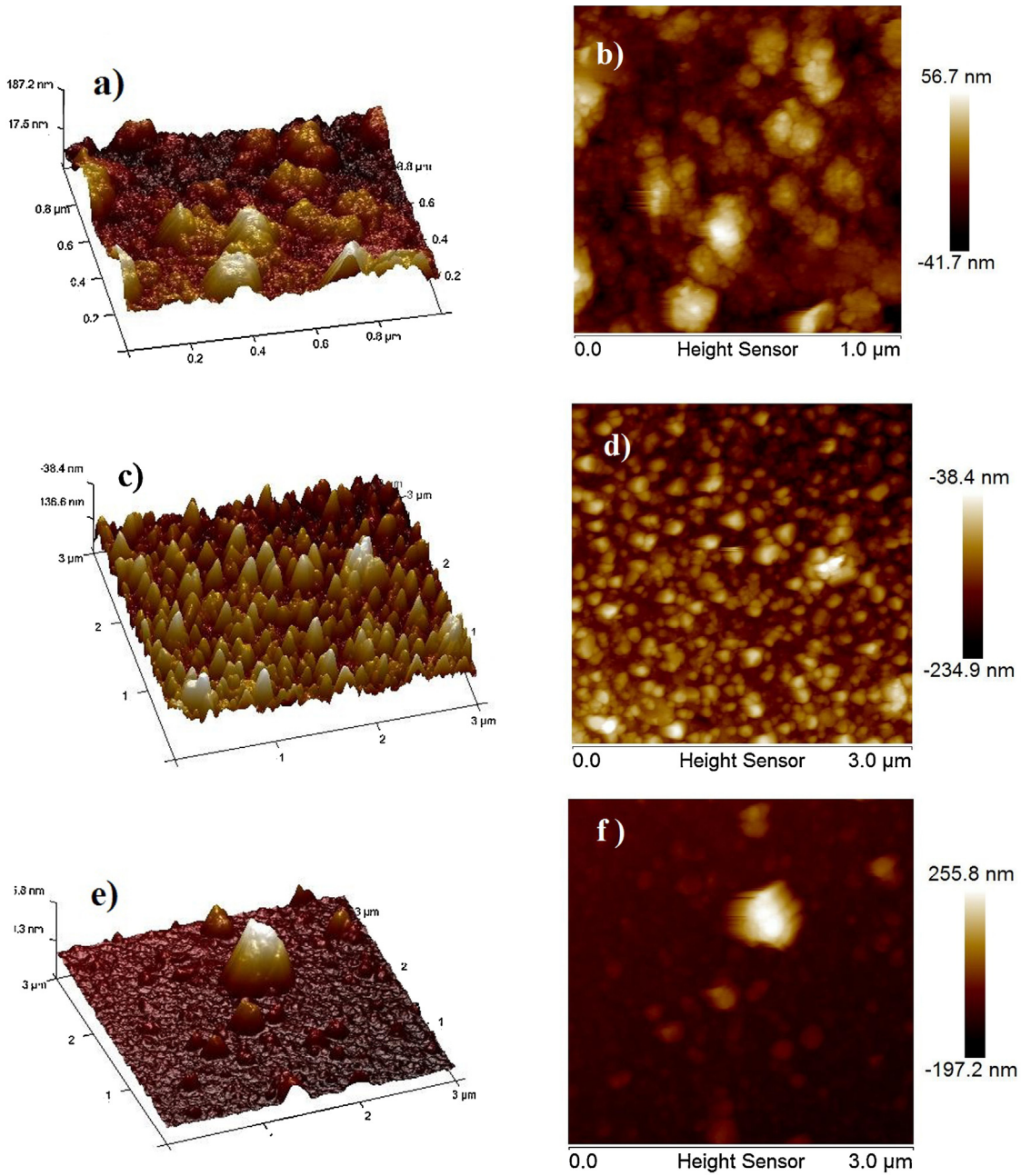

Fig. 2. AFM micrographs for the: as-prepared Bi_2S_3 thin films (a) 3D and (b) surface; annealed in air (c) 3D and (d) surface; and treated by argon plasma (e) 3D and (f) surface.

treatment is smoother than the thermally treated film, the plasma treatment would be better to this purpose. The different morphologies exhibited on the treated films can be understood considering the different temperatures of the treatment, in annealed in air was of 250 °C, while that for the plasma treatment was of 500 °C [19], then the carrier gas employed in plasma treatment have enough energy involved in the process to produce a higher impact on the surface, which it is observed in the sample treated in plasma (Fig. 2(e) and (f)).

4.2. Optical characterization

Fig. 3 displays the measurement of optical transmittance (T) and specular reflectance (R) of the samples: as-deposited, annealed in air at 250 °C and treated by Ar plasma. For the as-prepared films is found $T = 40\%$ at $\lambda = 1100$ nm and the absorption edge occurs at $\lambda \approx 735$ nm (see Fig. 3). It is clear from Fig. 3 that for samples annealed in air the value of T decreases up to 30% at $\lambda = 1100$ nm, due to the change of the amorphous phase into the crystalline phase, as it has been observed by XRD analysis. For the samples treated by Ar plasma, it found $T = 21\%$ at $\lambda = 1100$, this value is still lower than the above two cases, due to the combination of the change of the phase from amorphous to crystalline and its greater thickness compared with the obtained in air annealed film.

Plots presented in Fig. 4 correspond to (a) the absorption coefficient as a function of the photon energy (α *vs.* $h\nu$) and in the inset (b) $(\alpha h\nu)^{2/3}$ is plotted against $h\nu$. The energy band gap values of samples were determined from the plots of $(\alpha h\nu)^{2/3}$ vs. $h\nu$, by the extrapolated intercept on the $h\nu$ axis yields, which give the energy band gap value [20]. The values of the optical absorption coefficient of films in the visible region of the electromagnetic spectrum give to result higher than $1 \times 10^4\ cm^{-1}$, which would allow

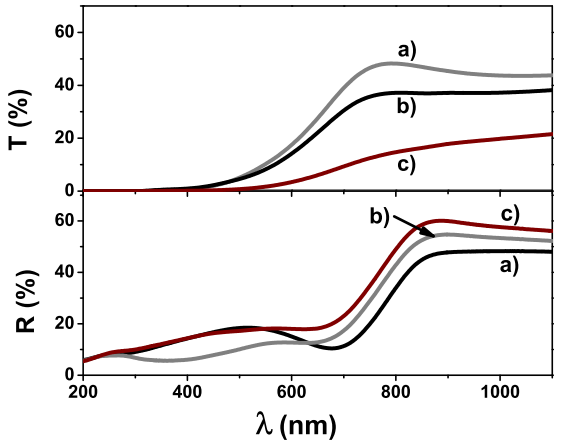

Fig. 3. Optical transmittance (T) and reflectance (R) spectra as a function of the wavelength in the range of 200–1100 nm for Bi_2S_3 thin film: (a) as-prepared, (b) annealed in air and (c) treated by Ar plasma.

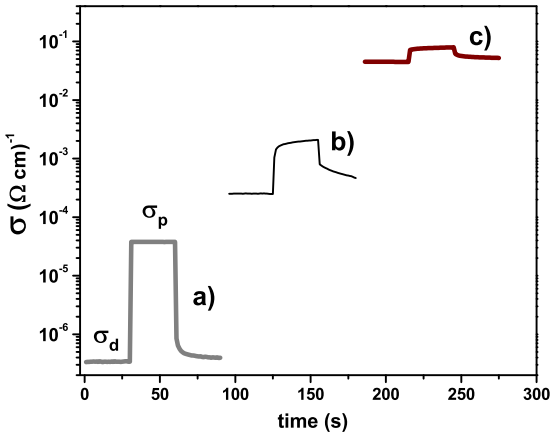

Fig. 5. Photoconductivity response plots for Bi_2S_3 thin films: (a) as-deposited, (b) annealed in air at 250 °C and (c) post-deposition treatment in argon plasma.

to these films absorb about 95% of the incident radiation with a thicknesses of the material with less than 200 nm, according to the Beer–Lambert law [21]. For the samples studied in this work, a direct forbidden transition was observed, since it was found $m = 2/3$ in all cases. The calculated value of E_g for the samples: as-deposited, annealed in air and treated by Ar plasma were: $E_g = 1.61$ eV (with a linear correlation coefficient $R = 0.999$); $E_g = 1.60$ eV ($R = 0.999$) and $E_g = 1.56$ eV ($R = 0.999$) respectively. The E_g value obtained for the plasma treated sample (1.56 eV) is better that the thermally annealed sample because its band gap is close to the optimal band gap for absorbing materials (1.1–1.6 eV). The increase in direct band gap may be due to the high crystalline order and larger grain size of films as revealed by XRD patterns, which it can produce a high carrier concentration [22].

4.3. Electrical characterization

Fig. 5 displays the photoconductivity response for the as-prepared Bi_2S_3 thin films, thermal annealing in air and treated by Ar plasma. The electrical conductivity (σ) under illumination is $3.6 \times 10^{-5}\,(\Omega\,\mathrm{cm})^{-1}$, $2.0 \times 10^{-3}\,(\Omega\,\mathrm{cm})^{-1}$ and $7.70 \times 10^{-2}\,(\Omega\,\mathrm{cm})^{-1}$ respectively. From the hot point tests, an n-type conductivity for thermally annealing in air and treated by Ar plasma thin films can be deduced. The electrical photoconductivity for the as-prepared films was $\sigma_p = 3.6 \times 10^{-5}\,(\Omega\,\mathrm{cm})^{-1}$; an increase of about two orders of magnitude was observed for samples annealed in air at 250 °C ($\sigma_p = 2.0 \times 10^{-3}\,(\Omega\,\mathrm{cm})^{-1}$) compared with the as-prepared films. The highest value of electrical photoconductivity was obtained for the samples treated by Ar plasma ($\sigma_p = 7.7 \times 10^{-2}\,(\Omega\,\mathrm{cm})^{-1}$). The increase in electrical conductivity of the films can be attributed to an increase in electron density, percolation effects due to porosity, surface degradation/etching, produced by the increase in surface roughness (see AFM analysis), and where some structural changes related to crystallinity occurs like a high grain size as revealed by XRD patterns, which increment charge trapping in the bulk. Perhaps some other reasons why the electrical resistivity decreases need to be further investigated.

The proper conductivity is between 0.001 and $0.1\,(\Omega\,\mathrm{cm})^{-1}$ because it creates greater depletion region (W), so the conductivity of the thin films treated by Ar plasma satisfy this requirement.

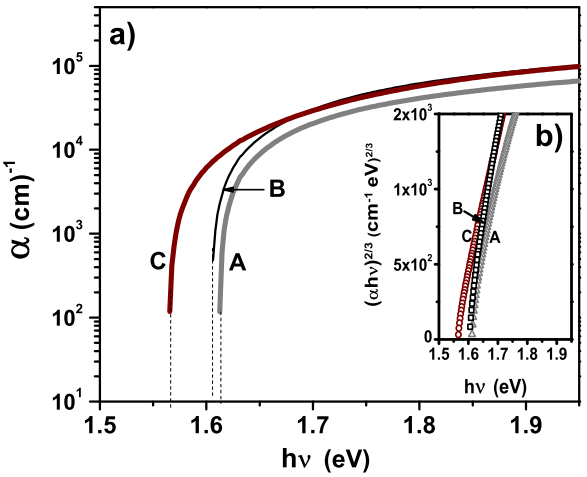

Fig. 4. (a) Optical absorption coefficient (α) as a function of the photon energy ($h\nu$) for the Bi_2S_3 thin films: (A) as-prepared, (B) annealed in air at 250 °C and (C) post-deposition treatment in argon plasma. Inset: (b) Determination of the E_g values for these films.

5. Conclusions

The results of this work show that the post-deposition treatment by Ar plasma is a viable alternative to enhance the optical, electrical, morphological and structural properties of Bi_2S_3 semiconductor thin film. The main advantage of this type of post-deposition treatment is the reduction of losses in thickness of the Bi_2S_3 films. Through the XRD analysis the change of the amorphous phase to crystalline phase was found for both post deposition treatments (thermal and plasma), since in both cases XRD patterns match well with the standard pattern of mineral bismuthinite (PDF # 17-0320). The measurements of the surface morphology by AFM analysis have shown that a significant improvement in lowering the roughness of the samples subjected to a treatment by plasma. The E_g values of the samples were 1.61 eV for the as-prepared films, 1.60 eV for thermally annealing in air and 1.56 eV for the films treated by Ar plasma. In the plasma treatment can be observed a substantially improvement in the optical properties of the Bi_2S_3 thin films. The E_g value obtained for the plasma treated sample is closer to the optimal band gap for absorbing materials. The conductivity of the films treated by plasma allows the formation of a wider area in depletion region, which involve a collection of charge carriers. We hope that the present work inspires further researches to combine the chemical deposition of Bi_2S_3 thin films and the post-deposition plasma treatment, to develop photovoltaic structures type TCO:CdS/Bi_2S_3-(P)/PbS in order to improve these type solar cells.

Acknowledgements

We are grateful to Patricia E. Altuzar Coello for the XRD measurements, Gildardo Casarrubias for the AFM measurements, J. Campos Álvarez for electrical characterization, O. Flores H.H. Hinojosa and F. Castillo for technical assistance. We also want to acknowledge the support of projects LYFYCS-CONACYT 123122 and CONACYT 128714. Harumi Moreno-García is grateful to DGAPA-UNAM for the postdoctoral fellowship.

References

[1] G. Armin, Aberle, Thin-film solar cells, Thin Solid Films 517 (2009) 4706–4710.
[2] C.H. Henry, Limiting efficiencies of ideal single and multiple energy gap terrestrial solar cells, J. Appl. Phys. 51 (1980) 4494.
[3] O. Madelung, Data in Science and Technology: Semiconductors Other than Group IV Elements and III–V Compounds, Springer-Verlag, Berlin, 1992, pp. 50.
[4] M. Medles, N. Benramdane, A. Bouzidi, A. Nakrela, H. Tabet-Derraz, Z. Kebbab, C. Mathieu, B. Khelifa, R. Desfeux, Optical and electrical properties of Bi_2S_3 films deposited by spray pyrolysis, Thin Solid Films 497 (2006) 58–64.
[5] S. Subramanian, P. Chithra lekha, D. Pathinettam Padiyan, Inclusion of polyaniline in electrodeposited bismuth sulphide thin films: synthesis and characterization, Curr. Appl. Phys. 9 (2009) 1140–1145.
[6] M.E. Rincón, M. Sánchez, P.J. George, A. Sánchez, P.K. Nair, Comparison of the properties of bismuth sulfide thin films prepared by thermal evaporation and chemical bath deposition, J. Solid State Chem. 136 (1998) 167–174.
[7] S.T. Haaf, H. Sräter, R. Brüggemann, G.H. Bauer, C. Felser, G. Jakob, Physical vapor deposition of Bi_2S_3 as absorber material in thin film photovoltaics, Thin Solid Films 535 (2013) 394–397.
[8] K. Mageshwari, R. Sathyamoorthy, Nanocrystalline Bi_2S_3 thin films grown by thio-glycolic acid mediated successive ionic layer adsorption and reaction (SILAR) technique, Mater. Sci. Semicond. Process. 16 (2013) 43–50.
[9] P.K. Nair, L. Huang, M.T.S. Nair, H. Hu, E.A. Meyers, R.A. Zingaro, Formation of p-type Cu_3BiS_3 absorber thin films by annealing chemically deposited Bi_2S_3–CuS thin films, J. Mater. Res. 12 (1997) 651–656.
[10] H. Moreno-García, M.T.S. Nair, P.K. Nair, Chemically deposited lead sulfide and bismuth sulfide thin films and Bi_2S_3/PbS solar cells, Thin Solid Films 519 (2011) 2287–2295.
[11] A.J. MacLachlan, F.T.F. O'Mahony, A.L. Sudlow, M.S. Hill, K.C. Molloy, J. Nelson, S.A. Haque, Solution-processed mesoscopic Bi_2S_3:polymer photoactive layers, Phys. Chem. Chem. Phys. 15 (2014) 1019–1023.
[12] L. Yu-Cheng, L. Ming Way, Bi_2S_3 liquid-junction semiconductor-sensitized SnO_2 solar cells, J. Electrochem. Soc. 161 (2014) H1–H5.
[13] A.K. Rath, M. Bernechea, L. Martinez, F. Pelayo Garcia de Arquer, J. Osmond, Solution-processed inorganic bulk nano-heterojunctions and their application to solar cells, Nat. Photonics 6 (2012) 529–534.
[14] Y. Rodríguez-Lazcano, H. Martínez, M. Calixto-Rodríguez, A. Núñez Rodríguez, Properties of CuS thin films treated in air plasma, Thin Solid Films 517 (2009) 5951–5955.
[15] A. Gómez, H. Martínez, M. Calixto-Rodríguez, D. Avellaneda, P.G. Reyes, O. Flores, Modification of optical and electrical properties of chemical bath deposited SnS using O_2 plasma treatments, Appl. Surf. Sci. 275 (2013) 273–277.
[16] M. Calixto-Rodriguez, H. Martínez, Y. Peña, O. Flores, H.E. Esparza-Ponce, A. Sanchez-Juarez, J. Campos-Alvarez, P. Reyes, A comparative study of the physical properties of Sb_2S_3 thin films treated with N_2 AC plasma and thermal annealing in N_2, Appl. Surf. Sci. 256 (2010) 2428–2433.
[17] M.T.S. Nair, P.K. Nair, Photoconductive bismuth sulphide thin films by chemical deposition, Semicond. Sci. Technol. 5 (1990) 1225–1230.
[18] H.J. Lewerenz, A. Heller, F.J. DiSalvo, Relationship between surface morphology and solar conversion efficiency of WSe_2 photoanodes, J. Am. Chem. Soc. 102 (1980) 1877–1880.
[19] H. Martínez, O. Flores, J.C. Poveda, B. Campillo, Asphaltene erosion process in air plasma: emission spectroscopy and surface analysis for air-plasma reactions, Plasma Sci. Technol. 14 (2012) 303–311.
[20] D.K. Schroder, Semiconductor Material and Device Characterization, 3rd ed., John Wiley & Sons, Hoboken, 2006.
[21] J.M. Parnis, K.B. Oldham, Beyond the Beer-Lambert law: The dependence of absorbance on time in photochemistry, J. Photochem. Photobiol. A 267 (2013) 6–10.
[22] M.M. Bagheri-Mohagheghi, N. Shahthmasebi, M.R. Alinejad, A. Youssefi, M. Shokooh-Saremi, Solid State Sci. 11 (2009) 233–239.